A New Approach to Nonlinear Feedback Control for Suppressing Periodic Disturbances

Part 2. A Case Study

X. J. Jing, Z. Q. Lang, S. A. Billings and G. R. Tomlinson

Department of Automatic Control and Systems Engineering
The University of Sheffield
Mappin Street, Sheffield
S1 3JD, UK

Research Report No. 934
August 2006

A New Approach to Nonlinear Feedback Control for Suppressing Periodic Disturbances

Part 2. A Case Study

Xing-Jian Jing[1], Zi-Qiang Lang[1], Stephen A. Billings[1] and Geofrey R. Tomlinson[2]

1 Department of Automatic Control and Systems Engineering, University of Sheffield
2 Department of Mechanical Engineering, University of Sheffield
Mappin Street, Sheffield, S1 3JD, U.K.
{X.J.Jing, Z.Lang, S.Billings & g.tomlinson}@sheffield.ac.uk

Abstract: In part 1 of this paper some fundamental theoretical results for the design of a nonlinear feedback controller to suppress periodic exogenous disturbances were developed based on the frequency domain theory of nonlinear systems, and a general procedure for the controller design was proposed. In this study, Part 2 of the paper, the new approach and the theoretical results in Part 1 are demonstrated using a case study based on the design of an active vibration control system. Simulation results are given to illustrate the effectiveness of the new method and the advantage of the nonlinear feedback controller.

1. Introduction

In Part 1 (Jing *et. al.*, 2006) of this paper, a new nonlinear feedback control approach to suppression of periodic disturbances was proposed. The problem was divided into several fundamental issues and a series of fundamental theoretical results and techniques for addressing these basic issues were established and developed, based on the frequency domain theory of nonlinear systems. In Part 2 of this paper, a case study is provided to demonstrate how to apply the new approach and the theoretical results established in Part 1 to design a nonlinear feedback controller. A simple nonlinear feedback controller for a vibration control system is designed and analysed in detail according to the design procedure of the new approach proposed in Part 1. Simulation results verify the theoretical results and illustrate the effectiveness of the new approach.

2. Preliminaries

In Part 1 (Jing *et. al.*, 2006), a novel frequency domain analysis based nonlinear feedback control approach was proposed for SISO linear systems to suppress period exogenous disturbances. The considered systems can be described by the differential equation:

$$\sum_{l=0}^{L} C_x(l)D^l x + b\cdot u + e\cdot\eta = 0 \tag{1}$$

$$y = \sum_{l=0}^{L-1} C_y(l)D^l x + d\cdot u \tag{2}$$

where, $x, y, u, \eta \in \Re^1$ represent the system state, output, control input, and an exogenous disturbance input respectively; η is a known, bounded and periodical vibration which can be described by a multi-tone function $\eta(t) = \sum_{i=1}^{K} |F_i|\cos(\omega_i t + \angle F_i)$; L is a positive integer; D^l is an operator defined by $D^l x = d^l x / dt^l$. The control problem is:

Given a frequency ω_0 and a desired magnitude level of the output frequency response Y^* at this frequency, find a nonlinear state feedback control law

$$u = -\varphi(x, D^1 x, \ldots, D^{L-1} x) \tag{3}$$

such that

$$[Y(j\omega)Y(-j\omega)]_{(\omega_0,u)} \le Y^* \tag{4}$$

where, $\varphi(x, D^1 x, \ldots, D^{L-1} x)$ can be written into a general form as

$$\varphi(x, D^1 x, \ldots, D^{L-1} x) = \sum_{p=1}^{M} \sum_{l_1 \cdots l_p = 0}^{L-1} C_{p0}(l_1, \cdots, l_p) \prod_{i=1}^{p} D^{l_i} x \tag{5}$$

M is a positive integer representing the maximum degree of nonlinearity in terms of $D^i x(t)$ (i=0…L-1); $\sum_{l_1 \cdots l_{p+q}=0}^{L-1}(\cdot) = \sum_{l_1=0}^{L-1} \cdots \sum_{l_{p+q}=0}^{L-1}(\cdot)$. $C_{p0}(.)$ for p=1 are linear parameters, and the rest are nonlinear parameters. Let $C_{p0} = [C_{p0}(0,\cdots,0), C_{p0}(0,\cdots,1), \cdots, C_{p0}(\underbrace{L,\cdots,L}_{p})]$.

Substituting (3) into (1), the closed loop system can be written

$$\sum_{p=1}^{M} \sum_{l_1 \cdots l_p = 0}^{L} \overline{C}_{p0}(l_1, \cdots, l_p) \prod_{i=1}^{p} D^{l_i} x + e\cdot\eta = 0 \tag{6a}$$

$$\sum_{p=1}^{M} \sum_{l_1 \cdots l_p = 0}^{L-1} \widetilde{C}_{p0}(l_1, \cdots, l_p) \prod_{i=1}^{p} D^{l_i} x = y \tag{6b}$$

where,

$$\overline{C}_{10}(l_1) = C_x(l_1) - bC_{10}(l_1), \quad \widetilde{C}_{10}(l_1) = C_y(l_1) - dC_{10}(l_1)$$

$$\overline{C}_{p0}(l_1, \cdots, l_p) = -bC_{p0}(l_1, \cdots, l_{p+q}), \quad \widetilde{C}_{p0}(l_1, \cdots, l_p) = -dC_{p0}(l_1, \cdots, l_p),$$

for $p = 2\cdots M$, $l_i = 0\cdots L$, and $i = 1\cdots p+q$.

The nonlinear feedback control problem can be divided into several basic problems in Part 1 of the paper. These are: (a) Determination of the analytical relationship between the system output spectrum and the nonlinear controller parameters. (b) Determination of an appropriate structure for the nonlinear feedback controller. (c) Derivation of a range for the values of the controller parameters over which the stability of the closed loop nonlinear system is guaranteed. (d) Numerical implementation of the nonlinear feedback controller design. Some theoretical results and effective techniques to solve the basic problems for the controller design have been developed in Part 1 of this paper. Based on these results, a general procedure for the design and analysis of the nonlinear feedback controller has also been proposed, which includes five steps as follows:

(A) Determination of the structure of the nonlinear feedback controller in (3), including the largest nonlinearity order *M*, and which of the nonlinear controller parameters $C_{p0}(.)$ (p=2,…,M) are used for the design.
(B) Derivation of a region for the nonlinear controller parameters, which can ensure the stability of the nonlinear closed loop system.
(C) Derivation of the polynomial expression for the system output spectrum in terms of the controller parameters.
(D) Examination of the effectiveness of the involved nonlinear controller parameters.
(E) Determination of the desired values for the nonlinear controller parameters to achieve a control objective.

Following this general procedure, a case study is presented in the following sections, which involves designing a simple nonlinear feedback controller for an active vibration control system.

3. Active control of a vibration system

Consider a simple case of the model in (1) and (2), which can be written as

$$\begin{cases} M\ddot{x} = -Kx - a_1\dot{x} + (\eta + u) \\ y = Kx + a_1\dot{x} - u \end{cases} \quad (7)$$

This is the model of a vibration system studied in Daley *et.al.*(2006). Following the procedure in Section 2, a nonlinear feedback controller is designed as follows to suppress the effect of vibrations due to the external disturbance $\eta(t)$ to the system.

3.1 Determination of the structure of the nonlinear feedback controller

For this simple system, *M* is directly chosen to be 3, and all other nonlinear controller parameters are chosen to be zero except $C_{30}(111)=a_3$. Later analysis will show that this is a good choice.

The nonlinear feedback control law (3) now is

$$u = -a_3\dot{x}^3 \quad (8)$$

Substituting (8) into (7), the closed loop system is obtained as

$$\begin{cases} M\ddot{x} = -Kx - a_1\dot{x} - a_3\dot{x}^3 + \eta & (9a) \\ y = Kx + a_1\dot{x} + a_3\dot{x}^3 & (9b) \end{cases}$$

Note that system (9) is a very simple case of system (6), that is, L=2, $\overline{C}_{10}(2) = M$, $\overline{C}_{10}(1) = a_1$, $\overline{C}_{10}(0) = K$, $\overline{C}_{30}(111) = a_3$, $\overline{C}_{01}(0) = -1$ and $\widetilde{C}_{10}(1) = a_1$, $\widetilde{C}_{10}(0) = K$, $\widetilde{C}_{30}(111) = a_3$; All other parameters in model (6) are zero. Now the task for the nonlinear feedback controller design is to determine a_3 such that system (9) satisfies the control objective (4).

3.2 Derivation of the stability region for the parameter a_3

The stability of the closed loop system (9) implies not only the existence of a convergent Volterra series to approximate the system input output relationship but also defines a region for the nonlinear controller parameter a_3 over which the design of a_3 can be conducted. According to Theorem 1 in Part 1 of the paper, the following result can be obtained.

Theorem 1. Consider the closed loop system (9), and suppose the exogenous disturbance input satisfies $\|\eta(t)\| \le F_d$. The system is asymptotically stable to a ball $B_{F_d\sqrt{\lambda_{\min}(Q)^{-1}\varepsilon}}(X)$, if $a_3>0$ and additionally there exist $P=P^T>0$, $\beta > 0$ and $\varepsilon > 0$ such that

$$Q=\begin{bmatrix} -A^TP-PA-\varepsilon^{-1}PEE^TP & -\beta A^TC^T+PB-\beta PEE^TC^T \\ * & +2\beta CB-\varepsilon^{-1}\beta^2CEE^TC^T \end{bmatrix}>0 \tag{10}$$

Moreover, the closed loop system (9) without a disturbance input is global asymptotically stable if (10) holds with E=0. Where $A=\begin{bmatrix} 0 & 1 \\ -K/M & -a_1/M \end{bmatrix}$, $B=E=[0,1/M]^T$, $C=[0,1]$.

Proof. The state-space equation of system (9a) can be written as

$$\dot{X} = AX - B\phi + E\eta$$

where, $X=[x,\dot{x}]^T$, $\phi = a_3\sigma^3, \sigma = CX$.

Choose a Lyapunov candidate as:

$$V = X^TPX + \tfrac{\alpha}{2}\sigma^4 \tag{11}$$

where, $\alpha > 0$. Equation (11) further follows

$$\begin{aligned} \dot{V} &= X^TP\dot{X} + \dot{X}^TPX + 2\alpha\sigma^3C\dot{X} \\ &= X^T(A^TP+PA)X - 2X^TPB\phi + 2X^TPE\eta + \tfrac{2\alpha}{a_3}\phi C(AX - B\phi + E\eta) \\ &= X^T(A^TP+PA)X - 2X^TPB\phi + \tfrac{2\alpha}{a_3}\phi CAX - \tfrac{2\alpha}{a_3}\phi CB\phi + 2X^TPE\eta + \tfrac{2\alpha}{a_3}\phi CE\eta \end{aligned} \tag{12}$$

Let $Z=\begin{bmatrix} X \\ \phi \end{bmatrix}$, $T=\begin{bmatrix} PE \\ \frac{\alpha}{a_3}CE \end{bmatrix}$, and $\beta = \alpha/a_3$ then equation (12) follows

$$\begin{aligned} \dot{V} &= Z^T\begin{bmatrix} A^TP+PA & \beta A^TC^T-PB \\ * & -2\beta CB \end{bmatrix}Z + Z^TT\eta \le Z^T\begin{bmatrix} A^TP+PA & \beta A^TC^T-PB \\ * & -2\beta CB \end{bmatrix}Z + \varepsilon^{-1}Z^TTT^TZ + \varepsilon\eta^T\eta \\ &= Z^T\left(\begin{bmatrix} A^TP+PA & \beta A^TC^T-PB \\ * & -2\beta CB \end{bmatrix} + \varepsilon^{-1}TT^T\right)Z + \varepsilon\eta^2 = -Z^TQZ + \varepsilon\eta^2 \end{aligned} \tag{13}$$

Note that, in the inequality above, the following inequality is used

$$2Z^TT\eta \le \varepsilon^{-1}Z^TTT^TZ + \varepsilon\eta^T\eta, \text{ for any } \varepsilon > 0.$$

If inequality (10) holds, then $Q=Q^T>0$, therefore $Z^TQZ \ge \lambda_{\min}(Q)\|X\|^2$ is a K-function of $\|X\|$. Hence, according to Theorem 1 in Part 1 of the paper (Jing *et.al.* 2006), the system is asymptotically stable to a ball $B_\rho(X)$ with $\rho = \sqrt{\lambda_{\min}(Q)^{-1}\varepsilon\sup(\|\eta\|^2)} = F_d\sqrt{\lambda_{\min}(Q)^{-1}\varepsilon}$. Additionally, when there is no exogenous disturbance input, and if (10) holds with E=0, then it is obvious that the system without a disturbance input is globally asymptotically stable. This completes the proof. □

With the guaranteed stability around zero equilibrium, the input output relationship of system (9) can be approximated by a convergent Volterra series. Thus the frequency domain theory of nonlinear systems based on Volterra series can be applied, provided that the system parameters satisfy the conditions of Theorem 1. However, it is noted that inequality (10) has no relation with a_3 and is determined by the linear part of system (9) which can be checked by using the LMI technique (Boyd et al. 1994). This implies that the value of a_3 has no effect on the stability of the system if the inequality (10) is satisfied. Hence, the nonlinear controller parameter a_3 is now only restricted to the region $[0,\infty)$.

3.3 Derivation of the polynomial representation of the system output spectrum

Note that only $C_{30}(111)=a_3$ and all other nonlinear parameters C_{p0} for $p>2$ are zero. According to Proposition 2 in Part 1 of this paper, the following parametric characteristics of the GFRFs can be obtained

$$CE(H_2^1(\cdot)) = C_{20} \oplus \sum_{p=2}^{\lfloor 2+1/2 \rfloor} C_{p0} \otimes CE(H_{2-p+1}^1(\cdot)) = C_{20} = 0\,,\quad CE(H_3^1(\cdot)) = C_{30} \oplus \sum_{p=2}^{\lfloor 3+1/2 \rfloor} C_{p0} \otimes CE(H_{3-p+1}^1(\cdot)) = C_{30} = a_3$$

$$CE(H_4^1(\cdot)) = C_{40} \oplus \sum_{p=2}^{\lfloor 4+1/2 \rfloor} C_{p0} \otimes CE(H_{4-p+1}^1(\cdot)) = 0\,,$$

$$CE(H_5^1(\cdot)) = C_{50} \oplus \sum_{p=2}^{\lfloor 5+1/2 \rfloor} C_{p0} \otimes CE(H_{5-p+1}^1(\cdot)) = C_{30} \otimes CE(H_3^1(\cdot)) = a_3^2\,,\ \cdots\cdots$$

It is easy to check from Propositions 2 and 3 in Part 1 of this paper that

$$CE(H_{2n+1}^1(\cdot)) = a_3^n \text{ for } n>0 \text{ and all other } CE(H_i^1(\cdot)) = 0\,. \tag{14}$$

This follows that only $H_{2n+1}^1(\cdot)$ for $n>0$ are nonzero and all others are zero. It should be noted that, if there are some other nonzero nonlinear controller parameters in C_{30}, then the conclusion still holds. The terms of the same order of nonlinearity order in C_{30} can be chosen properly in the feedback controller in order to increase the freedom of design and therefore improve the performance of the system output frequency response. This will be further discussed in other publications. In the present study, only the case where the control law u=-$a_3\dot{x}^3$ is considered for simplicity.

Using the parameter characteristics of the GFRFs, i.e., $CE(H_{2n+1}^1(\cdot)) = a_3^n$ for $n>0$, the parametric characteristics of the output spectrum of nonlinear system (9) can be obtained as

$$CE(Y(j\omega)) = CE(H_1^1(\cdot)) \oplus CE(H_2^1(\cdot)) \oplus \cdots \oplus CE(H_N^1(\cdot)) = \begin{bmatrix} 1 & a_3 & a_3^2 & \cdots & a_3^Z \end{bmatrix} \tag{15}$$

where, $Z=\lfloor N-1/2 \rfloor$. Therefore, the system output spectrum can be written as a polynomial expression as

$$Y(j\omega) = \overline{P}_0(j\omega) + a_3\overline{P}_1(j\omega) + a_3^2\overline{P}_2(j\omega) + \cdots + a_3^Z\overline{P}_Z(j\omega) \tag{16}$$

In order to check the validity of equation (16), the following the recursive computations are carried out according to Proposition 1 in Part 1 of this paper. It is easy to compute the GFRFs for (2n+1)th orders as follows:

$$H_1^1(j\omega_1) = 1 \Big/ \sum_{l_1=0}^{2} \overline{C}_{10}(l_1)(j\omega_1)^{l_1} = (M(j\omega_1)^2 + a_1(j\omega_1) + K)^{-1},$$

$$H_1^2(j\omega_1) = \sum_{l_1=0}^{2} \widetilde{C}_{10}(l_1) H_{11}^1(j\omega_1) = \left(a_1(j\omega_1) + K\right) H_1^1(j\omega_1)$$

$$H_3^1(j\omega_1,\cdots,j\omega_3) = -\frac{1}{e} H_1^1(j\omega_1+\cdots+j\omega_3) \sum_{p=2}^{3} \sum_{l_1\cdots l_p=0}^{L} \overline{C}_{p0}(l_1\cdots l_p) H_{3p}^1(j\omega_1,\cdots,j\omega_n)$$
$$= -H_1^1(j\omega_1+j\omega_2+j\omega_3)\cdot a_3 H_{33}^1(j\omega_1,\cdots,j\omega_3)$$
$$= -a_3 H_1^1(j\omega_1+j\omega_2+j\omega_3) H_1^1(j\omega_1) H_1^1(j\omega_2) H_1^1(j\omega_3)(j\omega_1)^1(j\omega_2)^1(j\omega_3)^1 := a_3 G_3^1$$

$$H_3^2(j\omega_1,\cdots,j\omega_3) = \sum_{p=1}^{3} \sum_{l_1\cdots l_p=0}^{L} \widetilde{C}_{p0}(l_1\cdots l_p) H_{3p}^1(j\omega_1,\cdots,j\omega_3)$$
$$= a_3 M H_1^1(j\omega_1+j\omega_2+j\omega_3) H_1^1(j\omega_1) H_1^1(j\omega_2) H_1^1(j\omega_3)(j\omega_1+\cdots+j\omega_3)^2(j\omega_1)^1(j\omega_2)^1(j\omega_3)^1$$

$$H_5^1(j\omega_1,\cdots,j\omega_5) = -(a_3)^2 H_1^1(j\omega_1+\cdots+j\omega_5)\begin{pmatrix} H_1^1(j\omega_1)H_1^1(j\omega_2)G_3^1(j\omega_3,\cdots,j\omega_5)(j\omega_1)(j\omega_2)(j\omega_3+j\omega_4+j\omega_5) \\ +H_1^1(j\omega_1)G_3^1(j\omega_2,\cdots,j\omega_4)H_1^1(j\omega_5)(j\omega_1)(j\omega_2+j\omega_3+j\omega_4)(j\omega_5) \\ +G_3^1(j\omega_1,\cdots,j\omega_3)H_1^1(j\omega_4)H_1^1(j\omega_5)(j\omega_1+j\omega_2+j\omega_3)(j\omega_4)(j\omega_5) \end{pmatrix}$$

$$H_5^2(j\omega_1,\cdots,j\omega_5) = a_3^2 M(j\omega_1+\cdots+j\omega_5)^2 H_1^1(j\omega_1+\cdots+j\omega_5)\cdot$$
$$\begin{pmatrix} H_1^1(j\omega_1)H_1^1(j\omega_2)G_3^1(j\omega_3,\cdots,j\omega_5)(j\omega_1)(j\omega_2)(j\omega_3+j\omega_4+j\omega_5) \\ +H_1^1(j\omega_1)G_3^1(j\omega_2,\cdots,j\omega_4)H_1^1(j\omega_5)(j\omega_1)(j\omega_2+j\omega_3+j\omega_4)(j\omega_5) \\ +G_3^1(j\omega_1,\cdots,j\omega_3)H_1^1(j\omega_4)H_1^1(j\omega_5)(j\omega_1+j\omega_2+j\omega_3)(j\omega_4)(j\omega_5) \end{pmatrix} := a_3^2 G_5^2$$

and so on. The system output spectrum can then be expressed as

$$\begin{aligned} Y(j\omega) &= \sum_{n=1}^{N} \frac{1}{2^{2n+1}} \sum_{\omega_{k_1}+\cdots+\omega_{k_{2n+1}}=\omega} H_{2n+1}^2(j\omega_{k_1},\cdots,j\omega_{k_{2n+1}}) F(\omega_{k_1})\cdots F(\omega_{k_{2n+1}}) \\ &= \frac{1}{2} H_1^2(j\omega)F(\omega) + \frac{a_3}{8} \sum_{\omega_{k_1}+\cdots+\omega_{k_3}=\omega} G_3^2(j\omega_{k_1},j\omega_{k_2},j\omega_{k_3}) F(\omega_{k_1})F(\omega_{k_2})F(\omega_{k_3}) \\ &\qquad + \frac{a_3^2}{32} \sum_{\omega_{k_1}+\cdots+\omega_{k_5}=\omega} G_5^2(j\omega_{k_1},\cdots,j\omega_{k_5}) F(\omega_{k_1})\cdots F(\omega_{k_5}) + \cdots \\ &:= \overline{P}_0(j\omega) + a_3\overline{P}_1(j\omega) + a_3^2\overline{P}_2(j\omega) + \cdots \end{aligned} \quad (17)$$

where

$$\overline{P}_0(j\omega) = \frac{1}{2} H_1^2(j\omega)F(\omega) = \frac{-j\left(a_1(j\omega)+K\right)F_d}{2M(j\omega)^2 + 2a_1(j\omega)^1 + 2K}, \quad \overline{P}_1(j\omega) = -\frac{3}{8} M F_d^3 \omega^5 \left|H_1^1(j\omega)\right|^2 \left[H_1^1(j\omega)\right]^2$$

$$\overline{P}_2(j\omega) = -\frac{3j}{32} M F_d^5 \left|j\omega H_1^1(j\omega)\right|^4 \left[j\omega H_1^1(j\omega)\right]^2 (j\omega)\cdot\left(j3\omega H_1^1(j3\omega) - j3\omega H_1^1(-j\omega) + j6\omega H_1^1(j\omega)\right)$$

These analytical expressions for $\overline{P}_i(j\omega)$ i=0,1,2… will be used in Section 4 to evaluate the values of the corresponding terms obtained by the numerical method in Step E of the design procedure to confirm the effectiveness of the design.

3.4 Examination of the effectiveness of the nonlinear parameter a_3

The effectiveness of the nonlinear term $a_3\dot{x}^3$ can be checked according to Proposition 4(2). That is, inequality $\Re(<\overline{P}_0(j\omega_0),\overline{P}_1(j\omega_0)>)<0$ can be used to check whether the simple nonlinear controller (11) is effective with respect to the control objective (4). From the results in Table 1, it is easy to show that $\Re(<\overline{P}_0(j\omega_0),\overline{P}_1(j\omega_0)>)$ = 0.5($\overline{P}_0(j\omega_0)\overline{P}_1(-j\omega_0)+\overline{P}_0(-j\omega_0)\overline{P}_1(j\omega_0)$)= -31.132<0 when a_3>0, ω_0 =8.1 rad/s and other system parameters as given in the simulation studies. Hence, the nonlinear control parameter a_3 is absolutely effective. If there are other nonlinear controller parameters, the same method can be used to check the effectiveness. Only the effective nonlinear terms are used in the controller. In fact, it can be further verified from Table 1 that $\overline{P}_n=\Re(\sum_{\substack{0\le i\le n-1\\ i\le j\le n, i+j=n}}<\overline{P}_i(j\omega),\overline{P}_j(j\omega)>)<0$ for all n=2k-1, k=1,2,3,…, and $|\overline{P}_n|<|\overline{P}_{n-1}|$. This implies that a_3 is effective for the whole stability region $[0,\infty)$ obtained in Section 2.2.

3.5 Determination of the desired value of the nonlinear parameter a_3

It follows from equation (16) that

$$\begin{aligned}Y(j\omega)Y(-j\omega)&=|Y(j\omega)|^2\\&=|\overline{P}_0(j\omega)|^2+a_3\left(\overline{P}_0(j\omega)\overline{P}_1(-j\omega)+\overline{P}_0(-j\omega)\overline{P}_1(j\omega)\right)+a_3^2(|\overline{P}_1(j\omega)|^2\\&\quad+\overline{P}_0(j\omega)\overline{P}_2(-j\omega)+\overline{P}_0(-j\omega)\overline{P}_2(j\omega))+\cdots\end{aligned}\tag{18}$$

Clearly, $|Y(j\omega)|^2$ is also a polynomial function of a_3. Given the magnitude of a desired output frequency response Y^* at any frequency ω_0, a_3 can be solved from (18) provided that $|Y(j\omega)|$ can be approximated by a polynomial expression of a finite order. However, in this case (18) with a lower order can not give a correct answer due to truncation errors. In order to solve this problem and to determine a desired value for a_3 to achieve the control objective (4), the numerical method proposed in Section 3.4 of Part 1 of this paper is used. Since (18) is a polynomial function of a_3, $|Y(j\omega)|^2$ can be directly approximated by a polynomial function of a_3 without computation of higher order GFRFs as follows:

$$Y(j\omega)Y(-j\omega)=|Y(j\omega)|^2\approx a_3^{2Z}\tilde{P}_{2Z}+\cdots a_3^n\tilde{P}_n+a_3^{n-1}\tilde{P}_{n-1}+\cdots+a_3\tilde{P}_1+|\overline{P}_0(j\omega)|^2\tag{19}$$

where $|Y(j\omega)|^2$ can be obtained through FFT of the data from simulations or experiments. Given 2*Z* different values of a_3, *i.e.*, a_{31}, a_{32}, …, $a_{3,2Z}$, (19) can be further written as

$$|Y(j\omega)_i|^2\approx a_{3i}^{2Z}\tilde{P}_{2Z}+\cdots a_{3i}^n\tilde{P}_n+a_{3i}^{n-1}\tilde{P}_{n-1}+\cdots+a_{3i}\tilde{P}_1+|\overline{P}_0(j\omega)|^2$$

for i=1,2,…,2Z, *i.e.*,

$$\begin{bmatrix}a_{31} & a_{31}^2 & a_{31}^3 & \cdots & a_{31}^{2Z}\\ a_{32} & a_{32}^2 & a_{32}^3 & \cdots & a_{32}^{2Z}\\ & & & \ddots & \vdots\\ a_{3,2Z} & a_{3,2Z}^2 & a_{3,2Z}^3 & \cdots & a_{3,2Z}^{2Z}\end{bmatrix}\cdot\begin{bmatrix}\tilde{P}_1\\ \tilde{P}_2\\ \vdots\\ \tilde{P}_{2Z}\end{bmatrix}=\begin{bmatrix}|Y(j\omega)_1|^2-|\overline{P}_0(j\omega)|^2\\ |Y(j\omega)_2|^2-|\overline{P}_0(j\omega)|^2\\ \vdots\\ |Y(j\omega)_{2Z}|^2-|\overline{P}_0(j\omega)|^2\end{bmatrix}$$

Then $\tilde{P}_1,\tilde{P}_2,\cdots,\tilde{P}_{2Z}$ are obtained as

$$\begin{bmatrix} \tilde{P}_1 \\ \tilde{P}_2 \\ \vdots \\ \tilde{P}_{2Z} \end{bmatrix} = \begin{bmatrix} a_{31} & a_{31}^2 & a_{31}^3 & \cdots & a_{31}^{2Z} \\ a_{32} & a_{32}^2 & a_{32}^3 & \cdots & a_{32}^{2Z} \\ & & & \ddots & \vdots \\ a_{3,2Z} & a_{3,2Z}^2 & a_{3,2Z}^3 & \cdots & a_{3,2Z}^{2Z} \end{bmatrix}^{-1} \cdot \begin{bmatrix} |Y(j\omega)_1|^2 - |\overline{P}_0(j\omega)|^2 \\ |Y(j\omega)_2|^2 - |\overline{P}_0(j\omega)|^2 \\ \vdots \\ |Y(j\omega)_{2Z}|^2 - |\overline{P}_0(j\omega)|^2 \end{bmatrix} \tag{20}$$

Consequently, equation (19) is obtained. Using this method, a polynomial expression of $|Y(j\omega)|^2$ in any order and of any accuracy can be achieved. Given a desired output frequency response Y^* at a frequency ω_0, a_3 can readily be solved from (19) to implement the design. Note that roots of equation (19) are multiple. According to Theorem 1, the solution a_3 should be a nonnegative real number.

4. Simulation Results

In this simulation study, the parameters of system (7) are: K=16000 N/m, a_1=296 N.S/m, M=240 Kg. The resonant frequency of the system is ω_0=8.1 rad/s. The disturbance input is $\eta(t) = F_d \sin(8.1t)$. In order to show the effectiveness and advantage of the nonlinear feedback controller (8), a substitutive linear controller $u = -a_2 \dot{x}$ will be used for comparison.

Firstly, let F_d=100 N. We need to obtain the polynomial function (19). In order to have a larger working region of a_3, let Z=6 in (19), and a_3= 500, 1000, 2000, 4000, 6000, 8000, 10000, 12000, 14000, 16000, 18000, 20000. Under these different values of a_3, the output frequency response of the system was obtained and the corresponding output spectrum was determined via FFT operations. Then $p_n(j\omega)$ for n=1…12 were obtained according to (20), which are summarized partly in Table 1. For comparisons, the corresponding theoretical results were also computed from equation (17) and are given partly in Table 1. From Table 1, it can be seen that there is a good match between the data analysis results and the theoretical computations although there are some errors. This result shows that the theoretical computation results are basically consistent with the results from the data analyses. It can also be seen from the data analysis results in Table 1 that equation (19) is in fact an alternative series in this case.

Figure 1 shows the results of the system output spectrum under different values of the nonlinear control parameter a_3 and provides a comparison between theoretical computations using polynomial expression (18) up to the 3rd order and the data analysis based results using the polynomial expression (19) up to the 12th order. This result demonstrates the analytical relationship between the nonlinear control parameter and the system output spectrum, and shows that the theoretical results have a good match with the data analysis results when a_3 is small since only up to the 3rd order GFRF are used in the theoretical computations. Hence, with an increase of a_3, the data analysis based method has to be used in order to give correct results. Moreover, it should be noted that the magnitude of the system output spectrum decreases with the increase of a_3. This verifies that the nonlinear control parameter a_3 is effective for the control problem.

Without a control input, the system output frequency spectrum is as shown in Fig 2, where $Y(j\omega)|_{\omega_0} = 335.71$. Note that the output response spectrum shown in the figures of this paper is 2|Y| not |Y|, which is also applied on the plot of the output spectrum using the theoretical computation. This is because 2|Y| represents the physical magnitude of the system output at the frequency ω_0. If the desired output frequency spectrum is set to be Y^*=180, then the calculation according to (19) and Theorem 2 yields a_3=11869. The output frequency spectrum under the nonlinear feedback control is as shown in Fig 3, where $Y(j\omega)|_{\omega_0} = 180.08$, and hence the result matches the desired result quite well. The system outputs in the time domain before and after nonlinear feedback control are given in Fig 4. It can be seen that the system steady state performance is considerably improved when the nonlinear controller is used. This verifies that the nonlinear feedback control law (8) is very effective, which is consistent with the theoretical analysis in Section 2.4.

In order to further demonstrate the advantage of the nonlinear feedback controller, consider a linear damping controller $u = -275\dot{x}$. Under this linear control input, the system output frequency response as shown in Fig 5 is similar to that achieved with the nonlinear controller. However, when F_d is increased to 200 N, the output frequency response is quite different under the two controllers. The nonlinear feedback controller results in a much smaller magnitude of output frequency response at frequency ω_0, referring to Fig 6 and Fig 7. Fig 8 shows the results of the system outputs in the time domain under the two different control inputs, indicating the nonlinear controller has a much better result than the linear controller. When the input frequency ω_0 is increased to be 15 rad/s, the same conclusions can be reached for the two controllers, referring to Fig 9 and Fig 10. When the input frequency is decreased to be 5 rad/s, the output spectrums under the two controllers are similar (see Fig 11 and Fig 12). The results demonstrate the advantage of the nonlinear feedback controller, and indicate that nonlinear feedback control can achieve better and more robust performances than a simple linear damping control for vibration suppression.

5. Conclusions

Through the design and analysis of a nonlinear feedback controller for a vibration control system, a new approach for the design of nonlinear feedback controllers for periodic disturbance suppression developed in Part 1 of this paper has been demonstrated. This study verifies the effectiveness of the new approach and shows that a simple nonlinear feedback controller can achieve an improved and more robust performance than a linear controller. Future studies will focus on more systematic investigations of the five important issues associated with the design of a nonlinear feedback controller and the applications of the new approach in the control of more complicated systems.

Acknowledgement

The authors gratefully acknowledge the support of the Engineering and Physical Science Research Council, UK and the EPSRC-Hutchison Whampoa Dorothy Hodgkin Postgraduate Award, for this work.

References

S. Daley, J. Hatonen, D.H. Owens, "Active vibration isolation in a 'smart spring' mount using a repetitive control approach", Control Engineering Practice, 14, 991–997, 2006

S. Boyd, L. E. Ghaoui, E. Feron, and V. Balakrishnan, Linear Matrix Inequalities in System and Control Theory. Philadelphia: the Society for Industrial and Applied Mathematics. 1994

X.J. Jing, Z.Q. Lang, S.A. Billings and G.R. Tomlinson. A New Approach to Nonlinear Feedback Control for Suppressing Periodic Disturbance, Part 1. Fundamental Theory. Submitted to IJC, 2006

Tables and Figures

TABLE I

COMPARISON BETWEEN SIMULATION AND THEORETICAL RESULTS

Data analysis results		Theoretical computation results	
$\left\|\overline{P}_0(j\omega)\right\|^2$	1.1270e+05	$\left\|\overline{P}_0(j\omega)\right\|^2$	1.1257e+05
$\widetilde{P}_1$	-58.9652	$\overline{P}_0(j\omega)\overline{P}_1(-j\omega) + \overline{P}_0(-j\omega)\overline{P}_1(j\omega)$	-62.2641
$\widetilde{P}_2$	0.0423	$\left\|\overline{P}_1(j\omega)\right\|^2 + \overline{P}_0(j\omega)\overline{P}_2(-j\omega) + \overline{P}_0(-j\omega)\overline{P}_2(j\omega)$	0.0615
$\widetilde{P}_3$	-2.3762e-005	—	—
$\widetilde{P}_4$	9.1382e-009	—	—
$\widetilde{P}_5$	-2.3593e-012	—	—
…	…	…	…

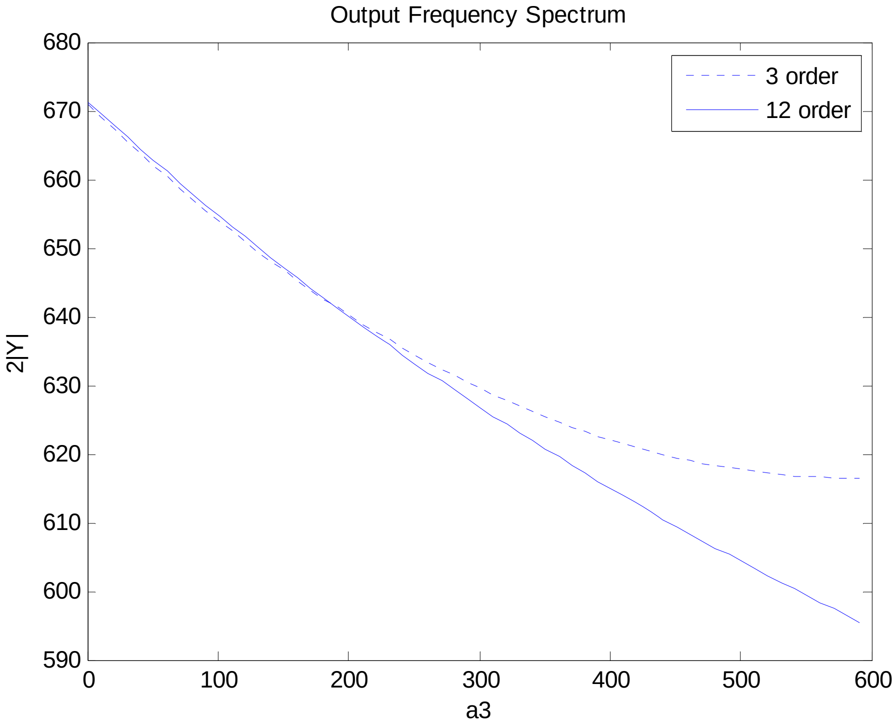

Fig. 1. Analytical relationship between the system output spectrum and the control parameter a_3

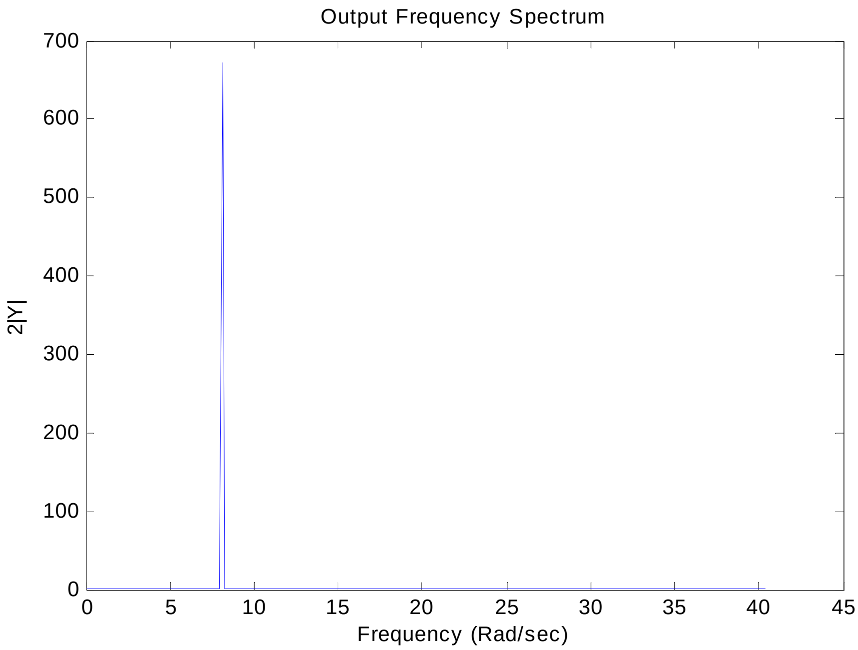

Fig. 2 Output spectrum without a feedback control

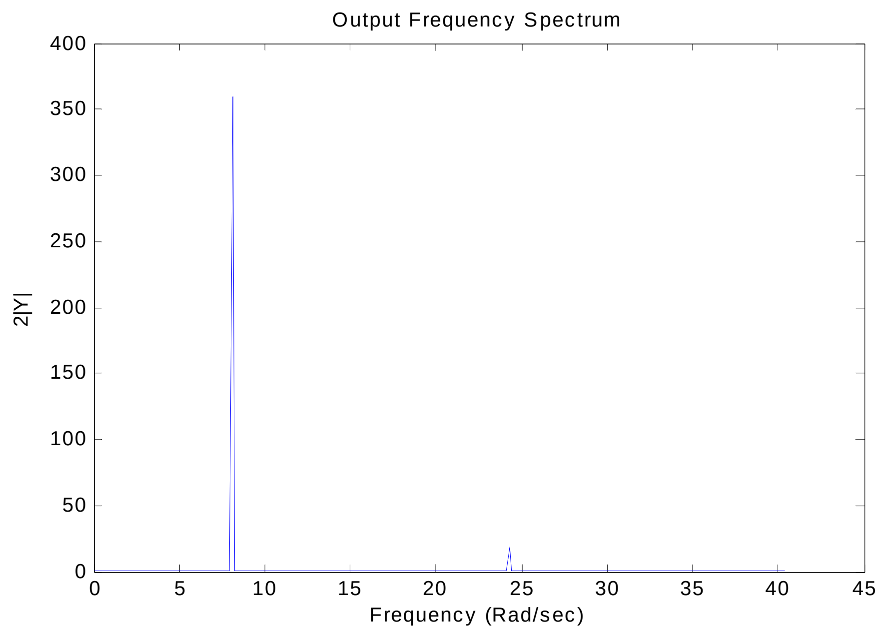

Fig. 3 Output spectrum with the designed nonlinear feedback control

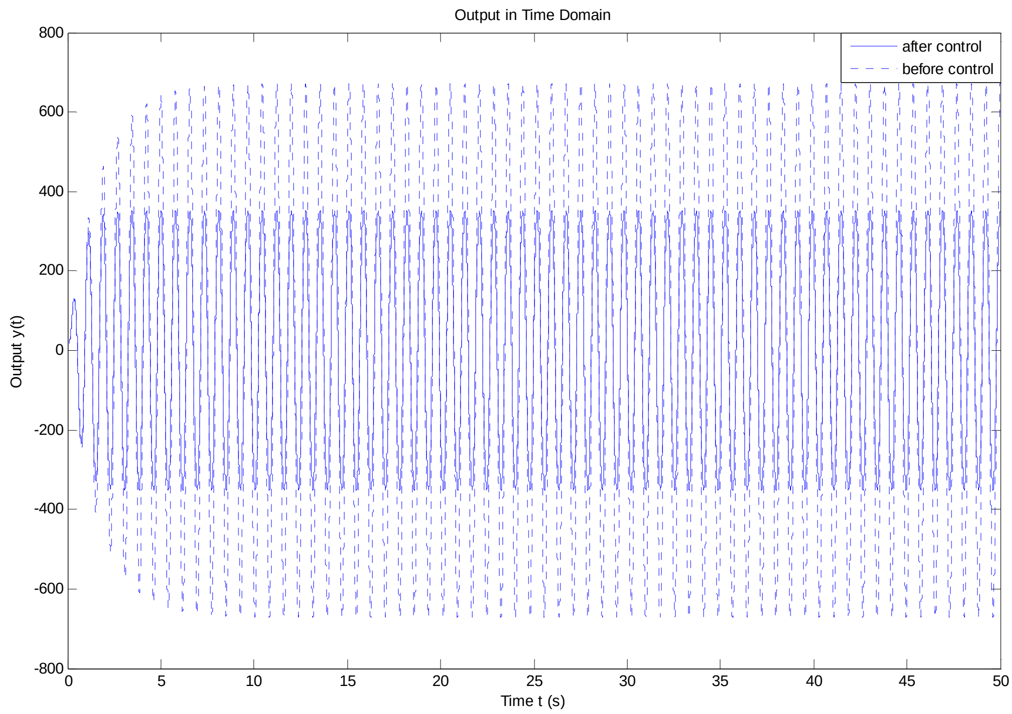

Fig. 4. System output in time domain: before and after control

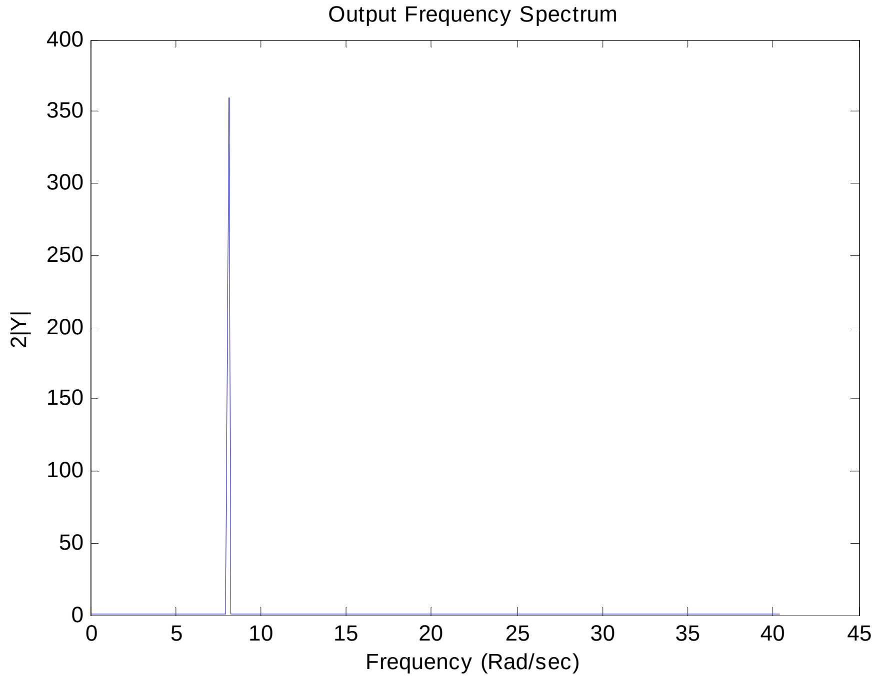

Fig. 5 Output spectrum with the linear feedback control

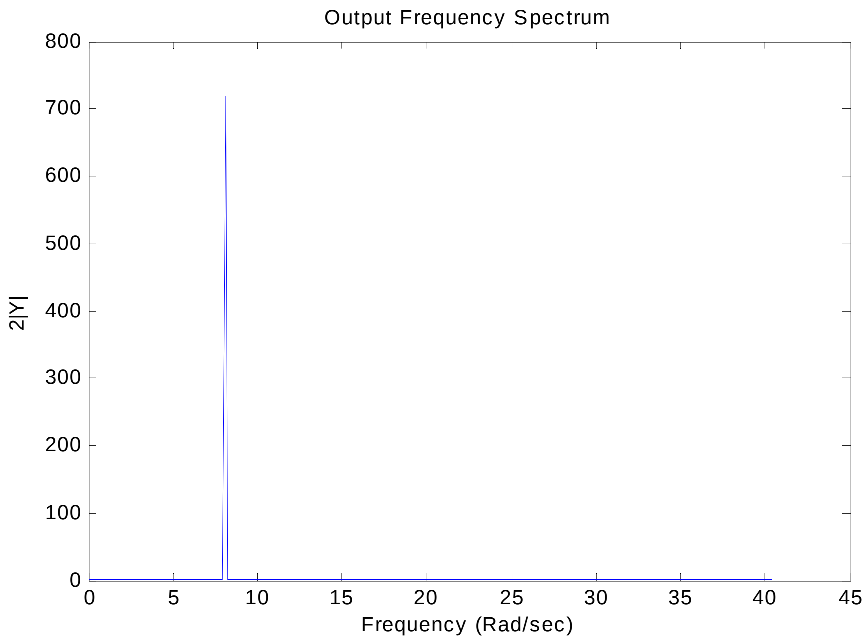

Fig. 6 Output spectrum with the linear feedback control when F_d is increased to F_d=200

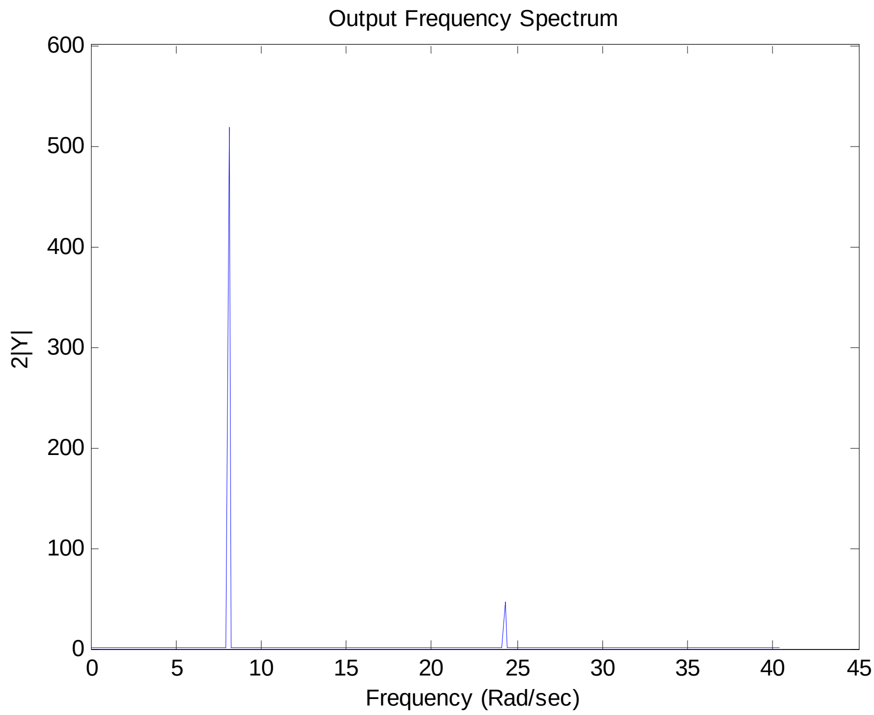

Fig. 7 Output spectrum with the designed nonlinear feedback control when F_d is increased to F_d=200

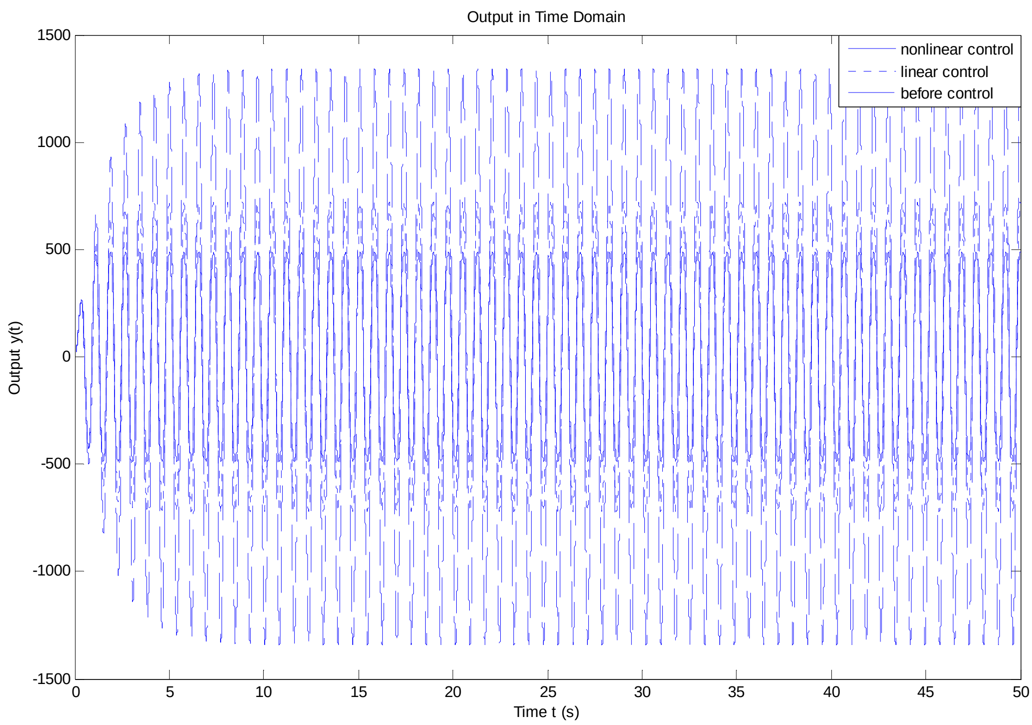

Fig. 8. The system outputs in time domain under different control inputs (F_d=200)

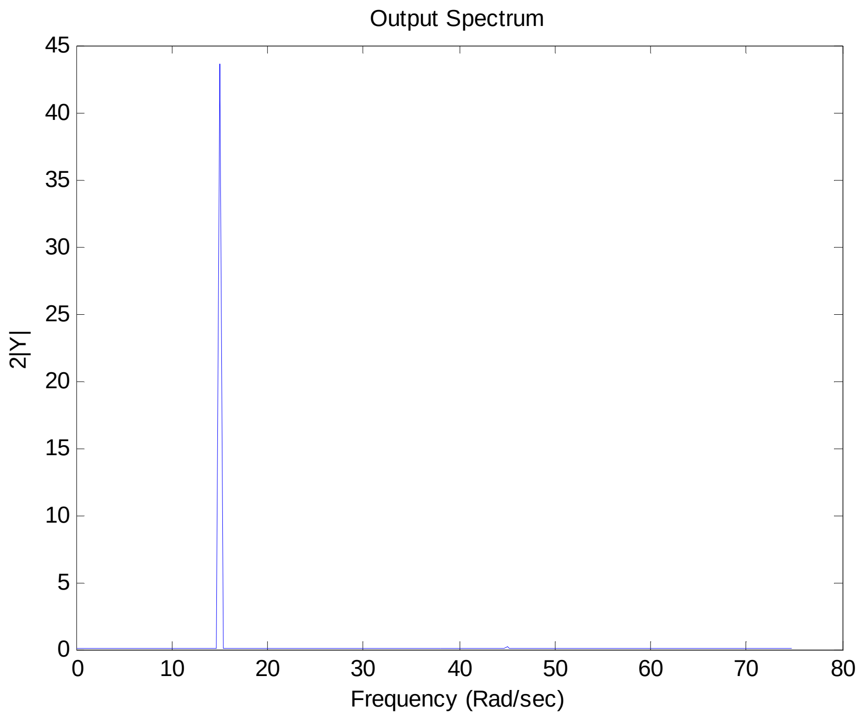

Fig. 9 Output spectrum with the designed nonlinear feedback control when $\omega_0 = 15$ rad/s, F_d=100

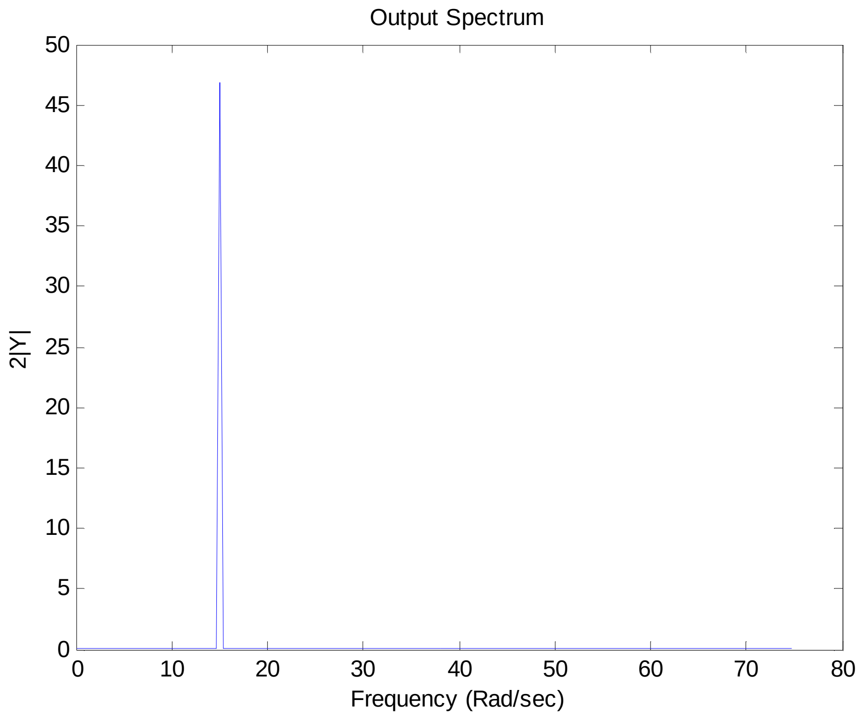

Fig. 10 Output spectrum with the linear feedback control when $\omega_0 = 15$ rad/s, F_d=100

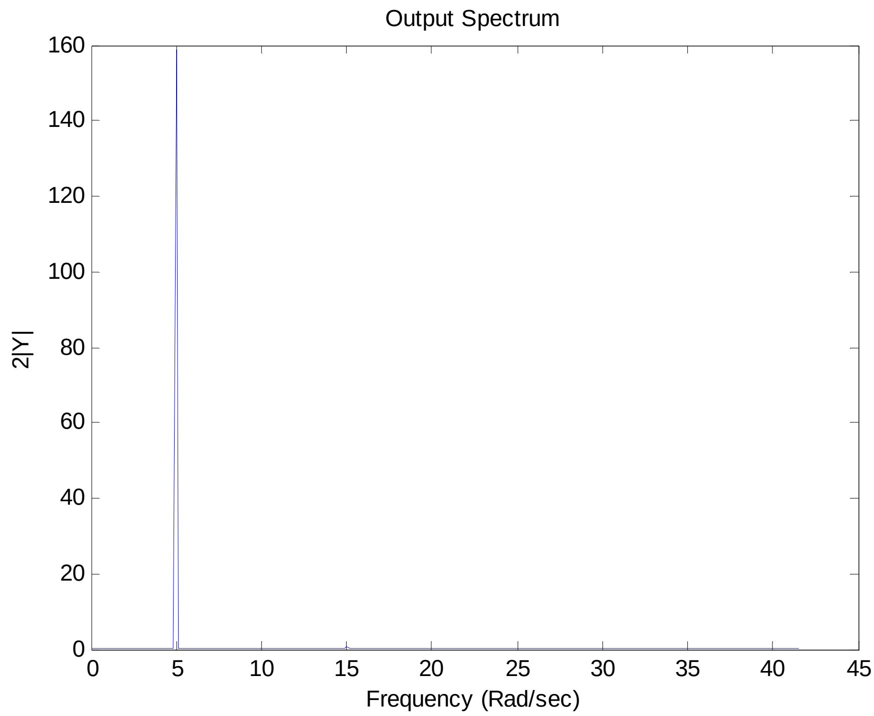

Fig. 11 Output spectrum with the designed nonlinear feedback control when $\omega_0 = 5$ rad/s, F_d=100

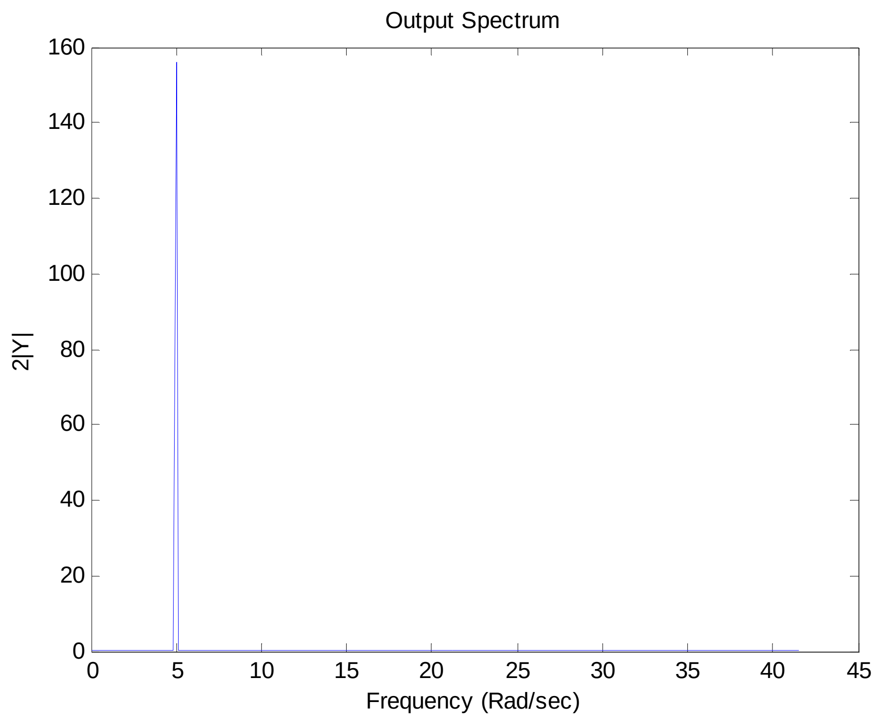

Fig. 12 Output spectrum with the linear feedback control when $\omega_0 = 5$ rad/s, F_d=100